Experimental Hematology 2019;77:6–11

BRIEF COMMUNICATION

Auer rod-like inclusions in the cytoplasm of B-cell lymphoma cells with bone marrow infiltration

Zhanxi Gao[a,1], Fang Cui[b,1], Mei Liu[a], Yukai Guo[a], Yuhong Hu[c], and Min Shi[a]

[a]*Department of Clinical Laboratory, Second Hospital of Hebei Medical University, Shijiazhuang, Hebei Province, China;* [b]*Department of Electron Microscope Laboratory Centre, Hebei Medical University, Shijiazhuang, Hebei Province, China;* [c]*Instrumental Analysis Center, Hebei Normal University, Shijiazhuang, Hebei Province, China*

(Received 8 April 2019; revised 10 July 2019; accepted 19 August 2019)

Auer rod-like inclusions are rarely seen in B-cell neoplasms patients. Here, we present a case of B-cell lymphoma with Auer rod-like inclusions in lymphoma cells. By light and transmission electron microscopy, these structures closely resembled Auer rods which were found in acute myeloid leukemia. The Auer rod-like inclusions were negative for cytochemical staining of MPO, α-naphthyl acetate esterase, and periodic acid–Schiff. Immunostaining and flow cytometric analysis confirmed monoclonal Kappa-positive malignant lymphocytes. Interestingly, the Auer rod-like inclusions exhibited diverse ultrastructural features, which ranged from fusiform, to needle-shape, to round, to crystalline cuboid, to long rod, to short rod and others; some were membrane structures, some membrane-free dense structures, and some lamellar structures. The patient was diagnosed with B-cell lymphoma with bone marrow infiltration.

Auer rods were first described in the cytoplasm of leukemia blasts by John Auer in 1906. Auer rods are commonly seen in myeloid progenitors, and serve as a diagnostic morphological feature of acute myeloid leukemia (AML) [1]. The differential diagnosis of hematopoietic neoplasms relies on the detection of cytoplasmic inclusions resembling Auer rods. Auer rod-like inclusions have been described in multiple myeloma [2], prolymphocytic leukemia (PLL) [3], B-cell acute lymphoblastic leukemia [4], chronic lymphocytic leukemia [4], splenic lymphoma [5], and nodal marginal zone lymphoma [6], and are quite distinct from the needle-shaped azurophilic Auer rods in AML. However, Auer rod-like inclusions are rarely seen in patients with B-cell neoplasms. Here, we present case of B-cell lymphoma with Auer rod-like inclusions in lymphoma cells.

Case

A 72-year-old man presented with a 1-week history of cough and fever. Physical examination revealed anemia, no yellowing of the skin and mucous membranes, and no bleeding spots or ecchymoses. Superficial lymph nodes were evident in both the neck and armpits; they were approximately 1×1 cm in size, active, smooth, soft, and not tender. Results of examinations of the head, ears, eyes, nose, and throat were negative. Chest computed tomography revealed evidence of previous tuberculosis. He had no history of allergies.

Laboratory workup revealed a red blood cell count of 2.1×10^{12}/L, hemoglobin of 77 g/L, platelet count of 88×10^{9}/L, and white blood cell count of 274.8×10^{9}/L; the differential count revealed lymphocytosis. Microscopy examination of a peripheral blood smear with Wright–Giemsa stain revealed mature lymphocytes with cytoplasm containing one to multiple Auer rod-like inclusions. A bone marrow aspirate and biopsy were performed for further evaluation before therapy.

Methods

Light microscopy

The bone marrow aspirates were stained with Wright–Giemsa, the cytochemical stains myeloperoxidase (MPO) and

Offprint requests to: Min Shi, Department of Clinical Laboratory, Second Hospital of Hebei Medical University, Shijiazhuang, Hebei Province 050000, China; E-mail: sm8344@sina.com

[1]ZG and FC contributed equally to this study.

0301-472X/
https://doi.org/10.1016/j.exphem.2019.08.003

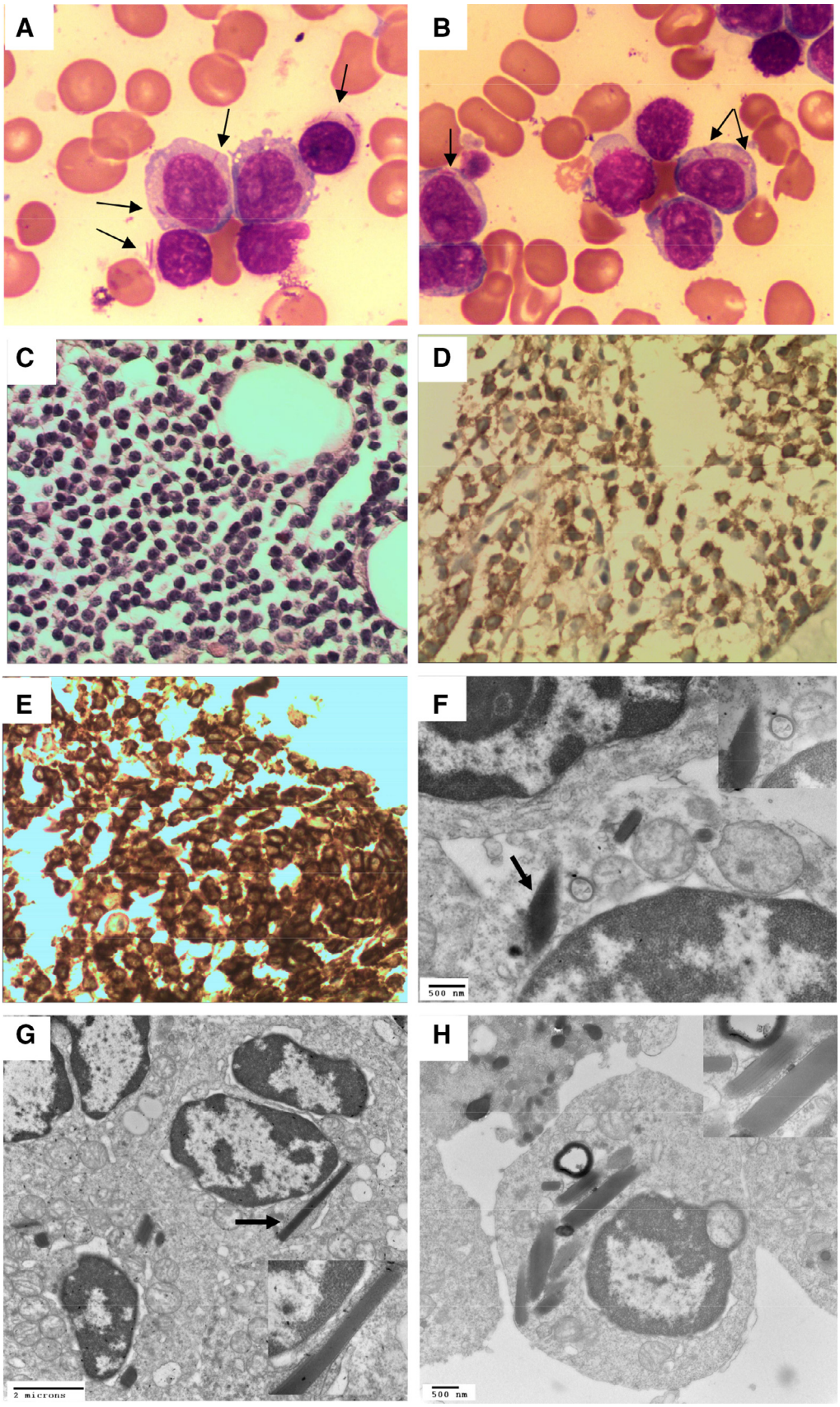
A
B
C
D
E
F
500 nm
G
2 microns
H
500 nm

α-naphthyl acetate esterase (α-NAE), and periodic acid–Schiff (PAS). The bone marrow biopsy was routinely processed with formalin fixation and was stained with hematoxylin and eosin. Immunohistochemical studies for CD19, CD20, CD5, CD3, CD10, CD11C, CD23, CyclinD1, BCL-6, SOX, and CD138 were also performed according to the manufacturer's directions.

Electron microscopy

Specimens collected from the bone marrow were fixed with 2.5% glutaraldehyde, followed by postfixation with osmium tetroxide. These specimens were then dehydrated, embedded in epoxy resin, and cut into ultrathin section. After double staining with uranyl acetate and lead citrate, the sections were observed with a transmission electron microscope.

Flow cytometric immunophenotyping

Cell suspensions were prepared and stained for flow cytometry within 24 hours of bone marrow aspiration sample collection. For the study, 50-μL aliquots of cell suspensions were incubated with fluorescent monoclonal antibodies, including CD45, CD19, CD20, CD22, Kappa, CD79b, FMC7, CD24, CD79a, CD5, CD2, cyCD3, CD11b, HLA-DR, CD11c, lambda, CD10, CD34, CD123, CD38, CD103, CD25, CD200, CD16, CD13, CD33, CD64, CD14, CD15, CD58, and CD45 (Becton Dickinson [BD] Biosciences, San Jose, CA). After 30 min, ammonium chloride (2.5 mL, 10 min) was added to lyse the red blood cells. The cells were pelleted and washed with phosphate-buffered saline containing 0.1% bovine serum albumin and 0.1% sodium azide. The second cell pellet was resuspended in 0.5 mL of phosphate-buffered saline containing 1% formaldehyde (electron microscope grade, Polysciences, Warrington, PA). Cells were analyzed on a FACSCalibur flow cytometer (BD Biosciences). Data were analyzed using CellQuest software (BD Biosciences).

Cytogenetic analysis

The chromosome specimens were obtained from bone marrow samples according to conventional methods following 24- and 48-hour cultures at 37°C. The images of chromosome karyotype were collected on a ZEISS imager Z2 (ZEISS, Oberkochen, Germany) and then analyzed by MetaClient (ZEISS, Oberkochen, Germany). When available, at least 20 metaphases were analyzed. Karyotypes of R-banding chromosomes were described according to the 2013 International System of Human Cytogenetic Nomenclature (ISCN 2013). Abnormal clones were defined as two or more cells with the same structural abnormality or the same extra chromosomes or the presence of three or more cells with loss of the same chromosome.

Reverse transcription polymerase chain reaction

Forty-three genes related to acute leukemia were detected by reverse transcription polymerase chain reaction. Cell suspensions were prepared from the bone marrow aspiration sample collection, and total RNA was extracted with Trizol reagent (Shanghai Yuanqi Biomedical Technology Co., Ltd, China). The cDNA was prepared from total RNA using a reverse transcription kit (Shanghai Yuanqi Biomedical Technology Co., Ltd, China) on a T100 Thermal Cycler (Bio-Rad, Hercules, CA, USA). Real-time polymerase chain reaction was performed to amplify each type of cDNA and was conducted with a fusion gene detection kit (Shanghai Yuanqi Biomedical Technology Co., Ltd, China) using a Roter-Gene Q fluorescence quantitative polymerase chain reaction instrument (Qiagen, Hilden, Germany).

Declaration of patient consent

The authors certify that they obtained all appropriate patient consent forms. On the form, the patient granted his consent for his images and other clinical information to be reported in this journal. The patient understands that his name and initials will not be published and due efforts will be made to conceal his identity, although anonymity cannot be guaranteed.

Results

Bone marrow aspiration revealed a hypercellular bone marrow with 63% mature-appearing lymphocytes. Most of the lymphocytes (20%–30%) with visible cytoplasm had one or more azurophilic, needle-shaped, slender, rod-shaped or coarse, and short rod-shaped inclusions resembling Auer rods (Figure 1A, B). Multicolor flow analysis showed that approximately 98% of the cells were lymphocytes composed primarily of CD19+ B cells, with Kappa-positive expression (CD19: 89.6%, CD20: 94.8%, CD22: 90.3%, Kappa: 92.8%, $CD79b^{dim}$: 86.6%, CD19+CD5+: 0.8%, FMC7: 6.8%, CD24: 96.6%, CD79a: 96.3%, CD19-CD5+: 1.6%, CD2: 7.8%, cyCD3: 1.9%, CD11b: 62.3%, HLA-DR: 49.1%, CD11c: 23.3%). The lambda, CD10, CD34, CD123, CD38, CD103, CD25, CD200, CD16, CD13, CD33, CD64, CD14, and CD15 phenotypes tested negative (Figure 2). Bone marrow biopsy revealed a hypercellular bone marrow (>90% cellularity) with diffuse lymphocytic infiltrates composed primarily of mature lymphocytes. Immunohistochemistry staining revealed that the lymphocytes were positive for CD19 and CD20 expression (Figure 1C–E). All cells were negative for CD3, CD5, DC10, CD11C, CD23, Bcl-6,

Figure 1. Morphological and immunohistochemistry results of bone marrow aspiration and biopsy. (**A, B**) Bone marrow smear revealing lymphocyte containing one or more azurophilic, needle-shaped, slender, rod-shaped or coarse, and short rod-shaped inclusions resembling Auer rods (*arrow*) (Wright–Giemsa, 1000×). (**C**) Bone marrow biopsy (BMx): Hypercellular bone marrow (>90% cellularity) with diffuse lymphocytic infiltrates with mostly small to medium-sized lymphocytes (hematoxylin and eosin, 400×). (**D**) CD19 was positive (400×). (**E**) CD20 was positive (400×). (**F**) Electron micrograph of Auer rod-like inclusions; the *arrow* indicates a fusiform structure with membrane-free dense structures (×30,000). The illustration in the right upper corner is amplified about three times (×100,000). (**G**) The *arrow* points to a needle-shaped structure, which was about 3 μm long in diameter (×15,000). The illustration in the right lower corner reveals electron density with membrane structures (×100,000). (**H**) Many electron-dense inclusions were fusiform, long-rod, and short-rod structures (×20,000). The illustration in the right upper corner reveals crystalline cuboid and lamellar structures with membrane structures (×100,000).

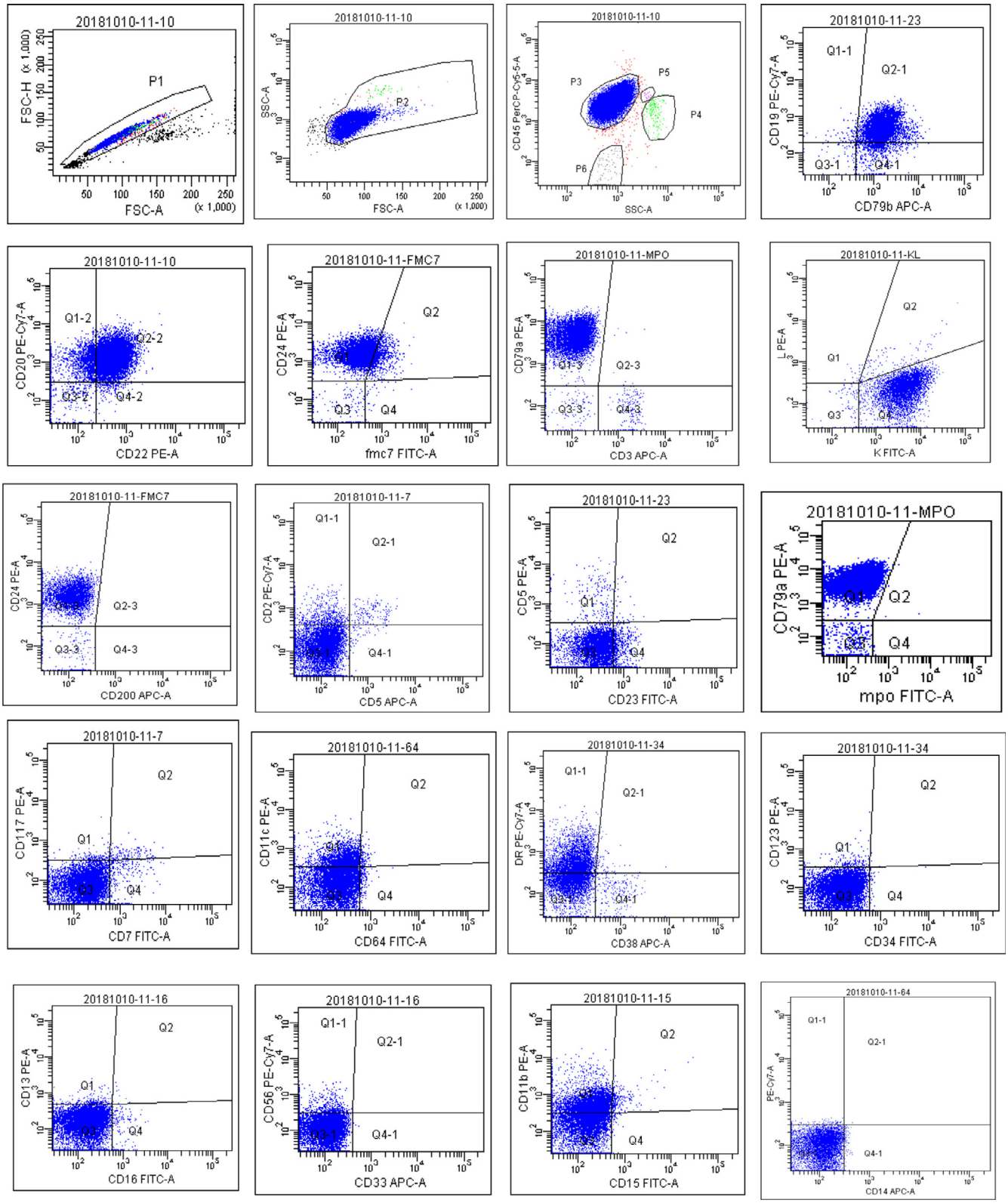

Figure 2. Flow analysis revealing that approximately 98% of the cells were lymphocytes composed primarily of CD19+ B cells, with Kappa-positive expression (CD19: 89.6%, CD20: 94.8%, CD22: 90.3%, Kappa: 92.8%, CD79b^{dim}: 86.6%, CD19+CD5+: 0.8%, FMC7: 6.8%, CD24: 96.6%, CD79a: 96.3%, CD19-CD5+: 1.6%, CD2: 7.8%, cyCD3: 1.9%, CD11b: 62.3%, HLA-DR: 49.1%, CD11c: 23.3%). The lambda, CD10, CD34, CD123, CD38, CD103, CD25, CD200, CD16, CD13, CD33, CD64, CD14, and CD15 phenotypes tested negative.

CyclinD1, SOX, and CD138 expression. The Auer rod-like inclusions were negative with the cytochemical stains MPO and α-NAE and PAS stain.

Cytogenetic analysis of the bone marrow aspirate revealed a normal metaphase karyotype of 46, XY [20]. Multiple reverse transcription polymerase chain reaction results were negative for fusion genes. Interestingly, the Auer rod-like inclusions exhibited diverse ultrastructural features, which ranged from fusiform, to needle-shaped, to round, to crystalline cuboid, to long rod, to short rod, and others; some were membrane structures, some membrane-free dense structures, and some lamellar structures (Figure 1F–H).

The patient was diagnosed with B-cell lymphoma with bone marrow infiltration (phase IV, group A). The recommended treatment was the CHOP (cyclophosphamide, doxorubicin, vincristine, and prednisone) regimen. However, the family refused treatment, and the patient left the hospital.

Discussion

Auer rod-like inclusions are rarely seen in nonmyeloid cells. Intracytoplasmic Auer rod-like inclusions have been described and are characteristic of various lymphoproliferative disorders [2–7]. It is difficult to morphologically differentiate these structures. Auer rods in myeloid cells are composed of fused lysosomes and contain peroxidase, lysosomal enzymes, and large crystalline inclusions. Myeloperoxidase staining is classically negative in these Auer rod-like inclusions, whereas true Auer rods stain intensely. The intracytoplasmic needle-like crystals in various lymphoproliferative disorders do not stain for MPO, SBB, PAS, or ACP [2–5].

In our case, these structures were single or multiple, needle-shaped, slender, rod-shaped or coarse, and short rod-shaped, and varied markedly in staining characteristics with Wright–Giemsa stain when examined by light microscopy. By light microscopy, these structures closely resembled the Auer rods found in AML. However, we could not find cytochemical evidence of lysosomal origin (results were negative for MPO, α-NAE, and PAS).

Cytochemical and electron microscopy evidence has confirmed that the Auer body is a lysosomal substance. Auer rod-like inclusions that have ultrastructural features strikingly similar to those of the Auer rods described in AML may be of abnormal lysosomal origin. Ultrastructurally, various forms of these inclusions have been described. Cytoplasmic inclusions that are crystalline, globular, tubular, or lamellar and either enclosed in subcellular membranes or free of membrane-dense structures have been described [8]. Djaldetti et al. [9] described a case of PLL with non-membrane-bound inclusions composed of crystalline protein. Kjeldsberg et al. [10] reported a case of PLL with small azurophilic granules surrounded by a smooth trilaminar membrane in the Golgi zone. The ultrastructural features of Auer rod-like inclusions in our case were fusiform, needle-shaped, round, crystalline cuboid, long rod, and short rod; some were membrane structures, some membrane-free dense structures, and some lamellar structures. We deduced, based on our experience, that it might have been a bacterial or mycoplasma product being degraded by autophagosomes. However, because of the lack of fresh tissues at the moment, further research using analytical electron microscopy or other technical means is needed concerning the composition of the Auer rod-like structures.

Auer rods are an important consideration in the differential diagnosis of myeloid neoplasms, as patient therapy and prognosis are significantly affected by the appropriate diagnosis. Moreover, ancillary studies, such as cytochemistry, flow cytometry, and immunohistochemistry, are critical in accurately recognizing the neoplastic cells as lymphocytes, rather than as immature myeloid cells. In this case, flow cytometry and immunohistochemistry revealed positive results for CD19, CD20, CD22, Kappa, and CD79, which further supported the diagnosis of B-cell lymphoma with bone marrow infiltration. However, the composition of the Auer rod-like structures was uncertain. B-Cell neoplasms with Auer rod-like inclusions are rare. The results of molecular cytogenetic examinations were all negative, which was important in the targeted therapy of a malignant hematological disorder.

Conclusions

Our case may indicate that there is a window of opportunity to identify neoplastic cells. Auer rods are often a useful morphologic finding. Nonetheless, cytochemical and immunochemical studies should be performed to avoid a misdiagnosis of malignant neoplasm. This case underscores the importance of incorporating all morphologic, histochemical, and immunophenotypic features into a pathologic diagnosis.

Acknowledgments

This research was supported by the Project of Science and Technology Department of Hebei Province under Grant No.16277734D.

Conflict of interest disclosure

The authors declare that there is no conflict of interest in relation to the publication of this article.

References

1. Yoshida Y, Oguma S, Ohno H. John Auer and Auer rods: Controversies revisited. Leuk Res. 2009;33:614–616.
2. Tejwani N, Tyagi S, Dass J. Multiple Auer rod like inclusions in multiple myeloma. Indian J Hematol Blood Transfus. 2017;33:121–122.

3. Juneja HS, Rajaraman S, Alperin JB, Bainton DF. Auer rod-like inclusions in prolymphocytic leukemia. Acta Haematol. 1987;77:115–119.
4. Dunphy CH, Chung D, Dunphy FR. Auer rod-like inclusions in adult common acute lymphoblastic leukemia. Hum Pathol. 1994;25:211–214.
5. Hristov AC, Saladino A, Nava VE, Gocke CD. Auer rod-like inclusions in a low-grade B-cell leukemia. Ann Diagn Pathol. 2010;14:292–295.
6. Zhu J, Zhang C, Guo W, Li F, Zou S, Pan B. Auer rod-like inclusions in the cytoplasm of splenic lymphoma cells. Leuk Lymphoma. 2014;55:2663–2664.
7. Takahashi T, Suzukawa M, Akiyama M, Hatao K. Auer rod-like cytoplasmic inclusion bodies in nodal marginal zone lymphoma cells. Int J Hematol. 2009;89:133–134.
8. Peters O, Thielemans C, Steenssens L, De Waele M, Hijmans W, Van Camp B. Intracellular inclusion bodies in 14 patients with B cell lymphoproliferative disorders. J Clin Pathol. 1984;37:45350.
9. Djaldetti M, Eisbruch A, Perek J, Hart J. Cytoplasmic inclusions of X-ray microprobe analysis in a case of prolymphocytic leukemia. J Cancer Res Clin Oncol. 1984;107:229–232.
10. Kjeldsberg CR, Bearman RM, Rappaport H. Prolymphocytic leukemia. An ultrastructural study. Am J Clin Pathol. 1980;l73:150–159.